COMPDYN 2015
5th ECCOMAS Thematic Conference on
Computational Methods in Structural Dynamics and Earthquake Engineering
M. Papadrakakis, V. Papadopoulos, V. Plevris (eds.)
Crete Island, Greece, 25–27 May 2015

A COMPUTATIONAL MODEL FOR LARGE-AMPLITUDE NONLINEAR VIBRATION OF CIRCULAR CMUTS UNDER PRIMARY RESONANCE

Aymen Jallouli, Najib Kacem*, Patrice Lemoal, Gilles Bourbon and Joseph Lardies

FEMTO-ST Institute - UMR 6174, Applied Mechanics Department
24, chemin de l'Épitaphe, F-25000 Besançon, France

*najib.kacem@femto-st.fr

Keywords: capacitive micromachined ultrasonic transducer (CMUT), nonlinear dynamics, harmonic blance method, asymptotic numerical method.

Abstract. *A computational multiphysics model for an electrically actuated clamped circular plate is developed. The Galerkin approach is used in order to transform the continuous model into a system having finite degrees of freedom. The discretized system is solved using the harmonic balance method (HBM) coupled with the asymptotic numerical method (ANM). The effects of the electrostatic excitation on the CMUT frequency responses are investigated for two set of design parameters. This model is an effective tool for MEMS designers to enhance the performances of CMUTs in term of generated acoustic power.*

1 INTRODUCTION

Recently, Capacitive Micromachined Ultrasonic Transducers (CMUTs) have attracted the attention of scientists and engineers and they are used in many applications such as generating 2D and 3D ultrasound images [1, 2], nondestructive evaluation [3] and developing capacitive pressure sensors [4]. Capacitive actuators have been used more extensively than piezoelectric ones due to their low mechanical impedance. Moreover, CMUTs can be produced with semiconductor fabrication techniques and they can be built on an Integrated Circuit (IC) while, for piezoelectric transducers, direct integration to IC is generally difficult. Another important benefit of CMUTs is the possibility to sustain to high temperatures which makes them suitable for high temperature applications such as automobile exhaust gas monitoring.

CMUTs are composed of two micro plates where the bottom electrode is fixed while the top electrode is vibrating. The distance between the two electrodes is called cavity. The vibration of the top electrode is due to the combination of the two electrostatic forces: a DC voltage deflects the microplate downward, and an AC voltage added to the bias voltage causing the vibration of the membrane which produces ultrasound waves. Several CMUT geometries have been proposed in the literature and Mendoza-Lopez et al. [5] proved that a circular CMUT has the highest displacement for the same voltage excitation.

Precise modeling of CMUTs is very important to build an optimized design and to understand its behavior. Among several modeling techniques, the Finite Element Method (FEM) is the most used one for CMUTs dynamics investigations [6, 7] or mathematical model validation [8]. Mason [9] suggested an equation of motion that describes the CMUT model assuming that the deflections at the operating point are small. Based on these equations, Ahrens et al. [10] used an equivalent electrical circuit for model simulations. Vogl et al. [11] developed an analytical reduced-order model for an electrically actuated clamped circular plate, taking into account the external forces and the residual stress. After determining the equation governing the plate, they studied the frequency response of the CMUT using the multiple scale method on the discretized model.

In this paper, a computational model for the nonlinear oscillations of circular CMUTs under primary resonance is developed. The continuous model includes Von Karman and electrostatic nonlinearities. The modal decomposition is used to transform the nonlinear partial differential equation into a finite degrees of freedom system which is numerically solved using the harmonic balance method (HBM) coupled with the asymptotic numerical method (ANM). Several numerical simulations have been performed in order to investigate the influence of design parameters on the frequency response of the considered MEMS. It is shown that the model enables the capture of all the nonlinear phenomena of the CMUT dynamics and describes the competition between the hardening and the softening behaviors. In practice, the proposed model can be used by CMUT designers in order to tune the impact of nonlinearities on the device performances.

2 PROBLEM FORMULATION

2.1 equations of motion

We consider a clamped circular microplate depicted in Figure 1, actuated by a static electric force $\tilde{V}_{dc}$ and an harmonic one $\tilde{V}_{ac}cos(\Omega\tilde{t})$. In this section, the model developed by Vogl and Nayfeh [11] is used. It describes the nonlinear dynamics of a circular, homogeneous and isotropic plate, using the following coupled partial differential equations:

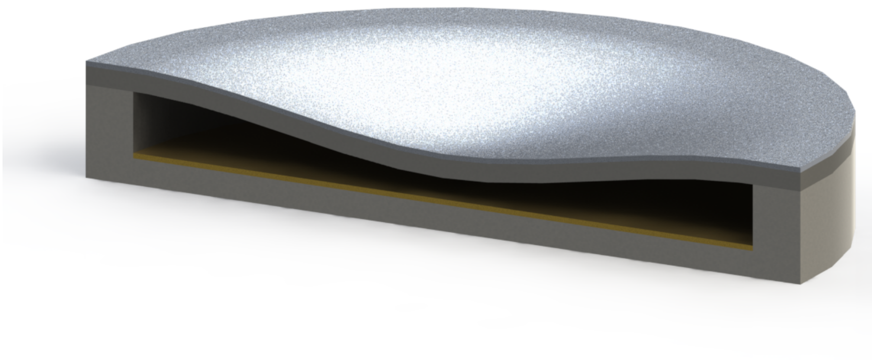

Figure 1: A schematic of a clamped circular plate electrostatically actuated.

$$\rho h \frac{\partial^2 \tilde{w}}{\partial \tilde{t}^2} + 2\tilde{c}\frac{\partial \tilde{w}}{\partial \tilde{t}} + D\tilde{\nabla}^4 \tilde{w} = \frac{1}{\tilde{r}}\frac{\partial}{\partial \tilde{r}}\left(\frac{\partial \tilde{w}}{\partial \tilde{r}}\frac{\partial \tilde{\Phi}}{\partial \tilde{r}}\right) + \tilde{\tau} h \nabla^2 \tilde{w} + \tilde{F} + \frac{\varepsilon_0 \tilde{v}^2\left(\tilde{t}\right)}{2(d-\tilde{w})^2} \tag{1}$$

$$\tilde{\nabla}^4 \tilde{\Phi} = -Eh\frac{\partial^2 \tilde{w}}{\partial \tilde{r}^2}\left(\frac{1}{\tilde{r}}\frac{\partial \tilde{w}}{\partial \tilde{r}}\right) \tag{2}$$

where

$$\tilde{\nabla}^4 = \left(\frac{\partial^2}{\partial \tilde{r}^2} + \frac{1}{\tilde{r}}\frac{\partial}{\partial \tilde{r}}\right)^2 \tag{3}$$

the tilde denotes a dimensional quantity, $\tilde{w}$ is the downward deflection, $\tilde{c}$ is a damping coefficient, ρ is the material mass density, h is the microplate thickness, $\tilde{\Phi}$ is the stress function, E is Young's modulus, D is the plate flexural rigidity defined as $D = \frac{Eh^3}{12(1-\nu^2)}$, ν is the Poisson's ratio, d is the effective gap distance between the top and bottom electrodes, ε_0 is the electric permittivity of the gap medium between the plate and electrode, $\tilde{\tau}$ is the residual stress, $\tilde{F}$ is an additional downward pressure, and $\tilde{v}\left(\tilde{t}\right)$ is the applied voltage. The boundary conditions of the vibrating circular plate are:

$$\begin{array}{c} \tilde{w}\left(R,\tilde{t}\right) = 0, \frac{\partial \tilde{w}\left(R,\tilde{t}\right)}{\partial \tilde{r}} = 0, \tilde{w}\left(0,\tilde{t}\right)\ is\ bounded \\ \frac{\partial^2 \tilde{\Phi}\left(R,\tilde{t}\right)}{\partial \tilde{r}^2} - \frac{\nu}{R}\frac{\partial \tilde{\Phi}\left(R,\tilde{t}\right)}{\partial \tilde{r}} = 0, \tilde{\Phi}\left(0,\tilde{t}\right)\ is\ bounded \end{array} \tag{4}$$

2.2 Normalization

We nondimensionalize the general equations according to:

$$\tilde{r} = Rr \qquad \tilde{t} = R^2\left(\frac{\rho h}{D}\right)^{1/2} t \qquad \tilde{w} = dw \qquad \tilde{c} = \frac{(D\rho h)^{1/2}}{R^2}c$$

$$\tilde{F} = \frac{Dd}{R^4}F \qquad \tilde{v}^2\left(\tilde{t}\right) = \frac{2Dd^3}{\varepsilon_0 R^4}v^2(t) \qquad \tilde{\tau} = \frac{D}{R^2 h}\tau \qquad \tilde{\Phi} = Ehd^2\Phi$$

The resulting dimensionless equation can be written as:

$$\frac{\partial^2 w}{\partial t^2} + 2c\frac{\partial w}{\partial t} + \nabla^4 w = \frac{\beta}{r}\frac{\partial}{\partial r}\left(\frac{\partial w}{\partial r}\frac{\partial \Phi}{\partial r}\right) + \frac{\tau}{r}\frac{\partial}{\partial r}\left(r\frac{\partial w}{\partial r}\right) + F(r,t) + \frac{v^2(t)}{(1-w)^2} \tag{5}$$

$$\nabla^4\Phi = -\frac{1}{r}\frac{\partial^2 w}{\partial r^2}\left(\frac{\partial w}{\partial r}\right) \tag{6}$$

where β is a nondimensional parameter defined as:

$$\beta = 12\left(1-\nu^2\right)d^2/h^2 \tag{7}$$

The nondimensional boundary conditions of the system are:

$$\begin{array}{c} w\left(1,t\right)=0, \frac{\partial w(1,t)}{\partial r}=0, w\left(0,t\right)\ is\ bounded \\ \frac{\partial^2\Phi(1,t)}{\partial r^2}-\nu\frac{\partial\Phi(1,t)}{\partial r}=0, \Phi\left(0,t\right)\ is\ bounded \end{array} \tag{8}$$

2.3 Reduced order model

The Galerkin procedure is used in order to transform Equations (5) and (6) into a system of finite number of ordinary-differential equations by letting

$$w\left(r,t\right)=\sum_{m=1}^{N}\eta_m\left(t\right)\phi_m(r) \tag{9}$$

where $\phi_m(r)$ is the m^{th} shape function, $\eta_m\left(t\right)$ is the m^{th} generalized coordinate, and N is the number of retained modes. Due to the symmetry of the problem, only the symmetric modes are considered. Following Nayfeh [12], the shape functions for a clamped circular plate actuated by symmetric forces can be written as:

$$\phi_m\left(r\right)=\frac{J_0(r\sqrt{\Omega_{\mathrm{m}}})}{J_0(\sqrt{\Omega_{\mathrm{m}}})}-\frac{I_0(r\sqrt{\Omega_{\mathrm{m}}})}{I_0(\sqrt{\Omega_{\mathrm{m}}})} \tag{10}$$

where J_0 and I_0 are respectively the first kind Bessel function and the modified Bessel function. The mode shapes are chosen orthonormal:

$$\int_0^1 r\phi_m(r)\phi_n(r)dr=\delta_{mn} \tag{11}$$

Substituting Equation (9) into Equations (5) and (6), multiplying by $\left(1-w\right)^2 r\phi_q(r)$ and integrating the resulting equation over $r\in[0,1]$, we obtain the following nonlinear system which is defined in the appendix.

$$M\left(\eta\right)\ddot{\eta}+2cM\left(\eta\right)\dot{\eta}+N\left(\eta\right)\eta=P\left(\eta\right)+v^2(t)L \tag{12}$$

where $M\left(\eta\right)$ and $N\left(\eta\right)$ are $N\times N$ nonlinear matrices and $P\left(\eta\right)$ is $N\times 1$ nonlinear vector defined in the appendix, $\eta\left(t\right)=\left\{\eta_1\left(t\right),\eta_2\left(t\right),\ldots,\eta_N\left(t\right)\right\}$ is a $N\times 1$ vector containing the generalized coordinates.

3 SOLVING PROCEDURE

Vogl and Nayfeh [11] used the multiple scale method to analyze the CMUT primary resonance associated to the first bending mode. Nevertheless, the obtained solutions are only valid for a low level of nonlinearity. Therefore, we propose a computational solving procedure based on the harmonic balance method (HBM) coupled with the asymptotic numerical method

(ANM), for which the solutions are valid up to very large displacement compared to the gap. This technique, proposed by Cochelin and Vergez [13], gives the periodic solutions of a dynamical system when a control parameter is varied. A periodic forced system could be written in the following form:

$$\dot{Y} = f(Y, \lambda) \tag{13}$$

where Y is a vector of unknowns, f a smooth vector valued function and λ a real parameter. The over-dot denotes differentiation with respect to time variable t. We applied the harmonic balance method on the system to decompose the solution $Y(t)$ into a truncated Fourier series.

$$Y(t) = Y_0 + \sum_{k=1}^{H} Y_{c,k} \cos(k\omega t) + Y_{s,k} \sin(k\omega t) \tag{14}$$

Substituting Equation (14) into Equation (13), we obtain an algebraic system with $2H + 1$ vector of unknowns Y_i, the unknown pulsation ω, and the parameter λ. The components of the Fourier series are collected into column vector U that contains all the unknowns Y_i with a size $(2H + 1)N_{eq}$; $U = [Y_0^T, Y_{c,1}^T, Y_{s,1}^T, \ldots, Y_{c,H}^T, Y_{c,H}^T]$ where N_{eq} is the number of equations in Equation (13). The latter is transformed into a quadratic one with $(2H + 1)N_{eq}$ and can be written as:

$$\omega M(U) = C + L(U) + Q(U, U) \tag{15}$$

where $M(.), C, L(.)$ and $Q(.,.)$ are operators which depend on $m(.), c, l(.)$ and $q(.,.)$. Once the algebraic system is obtained, we solve it using the asymptotic numerical method (ANM). To do so, Equation (15) is reformulated as:

$$R(U, \omega) = C + L(U) + Q(U, U) - \omega M(U) = 0 \tag{16}$$

As a first step, only the first bending mode is considered ($N = 1$). Equation (12) is reduced to:

$$\begin{aligned}
&(\ddot{\eta} + 2c\dot{\eta} + \Omega^2\eta) - 2(\ddot{\eta} + 2c\dot{\eta} + \Omega^2\eta)\eta A + (\ddot{\eta} + 2c\dot{\eta} + \Omega^2\eta)\eta^2 B \\
&= \beta\left[-\eta^3\left(C_1 + \tfrac{1+\nu}{1-\nu}C_2\right) + 2\eta^4\left(D_1 + \tfrac{1+\nu}{1-\nu}D_2\right) - \eta^5\left(E_1 + \tfrac{1+\nu}{1-\nu}E_2\right)\right] \\
&-\tau\eta F + 2\tau\eta^2 G - \tau\eta^3 H + I - 2\eta J + \eta^2 K + v^2(t)L
\end{aligned} \tag{17}$$

Equation (17) describes the dynamic behavior of the CMUT when considering only the first bending mode. In its quadratic form, Equation (17) can be written as:

$$\begin{aligned}
&\dot{a} = y \\
&\dot{y} = z \\
&0 = (\dot{z} + 2cy + \Omega^2 a) - 2(\dot{z} + 2cy + \Omega^2 a)aA + (\dot{z} + 2cy + \Omega^2 a)mB \\
&-\beta\left[-n\left(C_1 + \tfrac{1+\nu}{1-\nu}C_2\right) + 2an\left(D_1 + \tfrac{1+\nu}{1-\nu}D_2\right) - mn\left(E_1 + \tfrac{1+\nu}{1-\nu}E_2\right)\right] \\
&+\tau aF - 2\tau mG + \tau nH - I + 2aJ - mK - VVL \\
&0 = -m + aa \\
&0 = -n + ma \\
&0 = -V + V_{dc} + V_{ac}\cos(\omega t)
\end{aligned} \tag{18}$$

$$m\left(\dot{X}\right) = l_0(\omega) + l(X) + q(X, X) \tag{19}$$

where $X = (a, y, z, m, n, V)$ is the unknown vector of size $N_eq = 6$. Equation (19) is then implemented in MANLAB, an object-oriented MATLAB program which solves a quadratic system using the ANM [13].

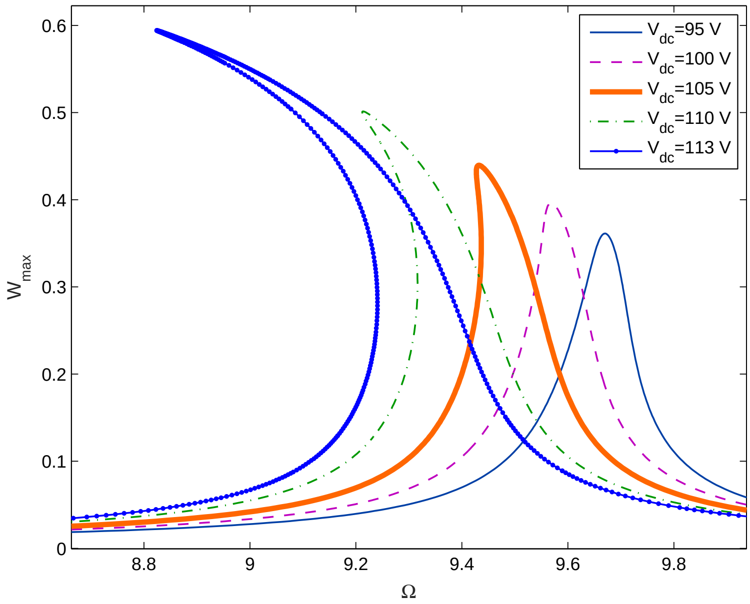

Figure 2: Forced frequency responses of the first CMUT design for $V_{ac} = 2V$ and several DC voltages. W_{max} is the out-of-plane normalized displacement of the membrane at its central point.

4 RESULTS AND DISCUSSION

In this section, several numerical simulations have been performed for two set of design parameters listed in Table 1 in order to investigate the effects of DC and AC voltages on the CMUT frequency responses under primary resonance.

For the first design, the ratio between the gap and the plate thickness is $d/h = 2$. Consequently, high DC voltages are needed to reach softening nonlinear behaviors. This is illustrated by Figure 2 which displays the evolution of the CMUT frequency response with respect to V_{dc} for $V_{ac} = 2V$. Since the excitation term is proportional to V_{dc}, increasing the DC voltage leads to an augmentation of the out-of plane displacement of the micro-plate $w(r, t)$. Moreover, the resonance frequency decreases due to the negative stiffness term which is proportional to V_{dc}^2. Remarkably, at a critical V_{dc}, the CMUT frequency response becomes nonlinear and the curve bends to the left (softening) due to the amplification of the electrostatic nonlinear terms.

Unlike the effect of V_{dc} on the CMUT frequency response, the variation of the AC voltage has a significant impact on the excitation amplitude and a negligible one on the negative electrostatic stiffness. Consequently, the resonance curves become more nonlinear when increasing V_{ac} without any remarkable frequency shift. This phenomena is displayed in Figure 3 for $V_{dc} = 50V$ where the frequency response exhibits a hardening behavior for $3V \leq V_{ac} \leq 6V$, since the geometric nonlinearities dominate the CMUT dynamics. Interestingly, for $V_{ac} = 7V$, the com-

Design	effective gap distance	plate thickness	plate radius	quality factor
1	$1\mu m$	$2\mu m$	$60\mu m$	50
2	$2\mu m$	$1\mu m$	$60\mu m$	50

Table 1: Design parameters of considered CMUTs

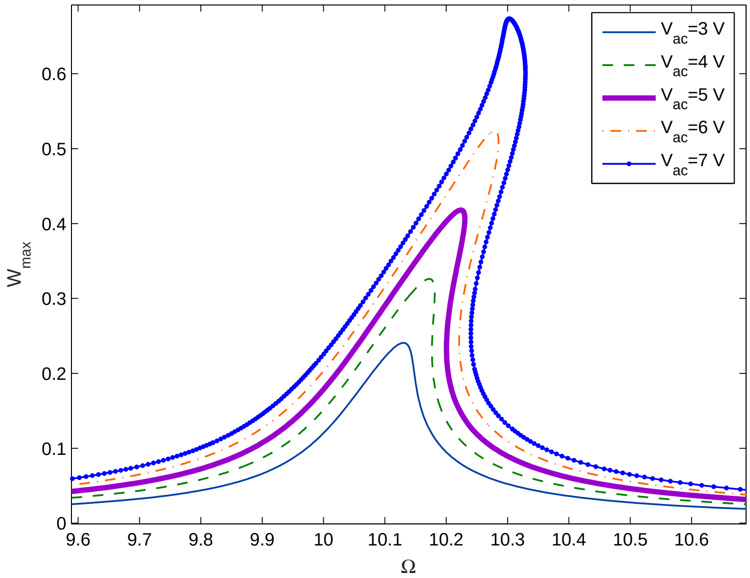

Figure 3: Forced frequency responses of the first CMUT design for $V_{dc} = 50V$ and several AC voltages.

petition between mechanical and electrostatic nonlinearities gives rise to a mixed hardening-softening behavior [14, 15, 16, 17] for which the displacement at the membrane center exceeded 60% of the gap.

The second design in Table 1 presents a larger gap with respect to the membrane thickness. Since the excitation amplitude is proportional to g^{-2} and compared to the first CMUT design, high DC voltages are needed in order to reach the softening behavior for $V_{ac} = 3V$ as shown in Figure 4. Moreover, the variation of the spring softening effect with respect to V_{dc} is slightly remarkable. Finally, Figure 5 displays the same phenomena described for the first design when V_{ac} is increased from $3V$ up to $11V$ and $V_{dc} = 100V$ for which the displacement at the membrane center is below 45% of the gap.

5 CONCLUSION

In this paper the nonlinear dynamics of circular CMUTs under primary resonance was investigated. The mathematical model, that takes into account the electrostatic and mechanical nonlinearities, is transformed into a set of coupled nonlinear ordinary differential equations using the Galerkin procedure. The harmonic balance method was then used to decompose the obtained system into a quadratic one which has been solved using the asymptotic numerical method. It has been shown that the DC voltage has a direct impact on the resonance frequency and the hardening or softening nonlinear effects while V_{ac} affects mostly the shape of the resonance curves. Moreover, depending on the chosen actuation voltages and the design parameters, the frequency response can switch between hardening, softening and mixed behaviors. In practice, the developed computational model can be used by MEMS designers to improve the performances of CMUTs in several applications such as High Intensity Focused Ultrasound (HIFU) in cancer therapy.

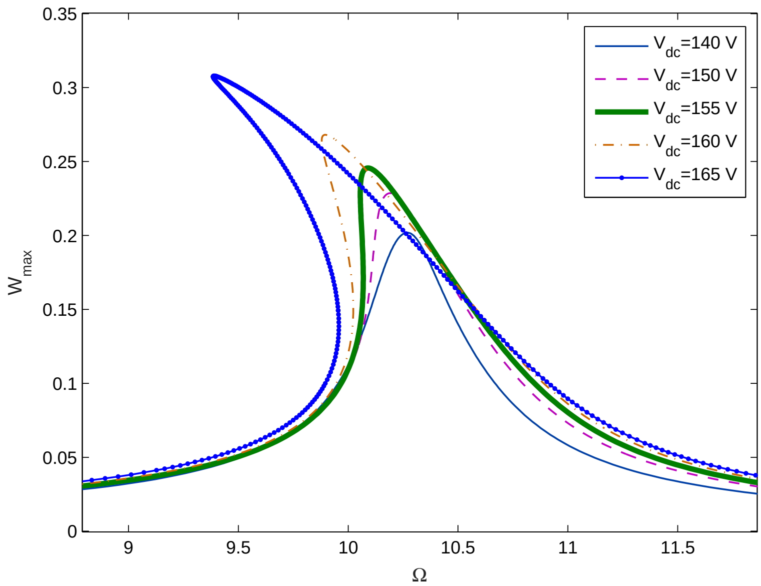

Figure 4: Forced frequency responses of the second CMUT design for $V_{ac} = 3V$ and several DC voltages.

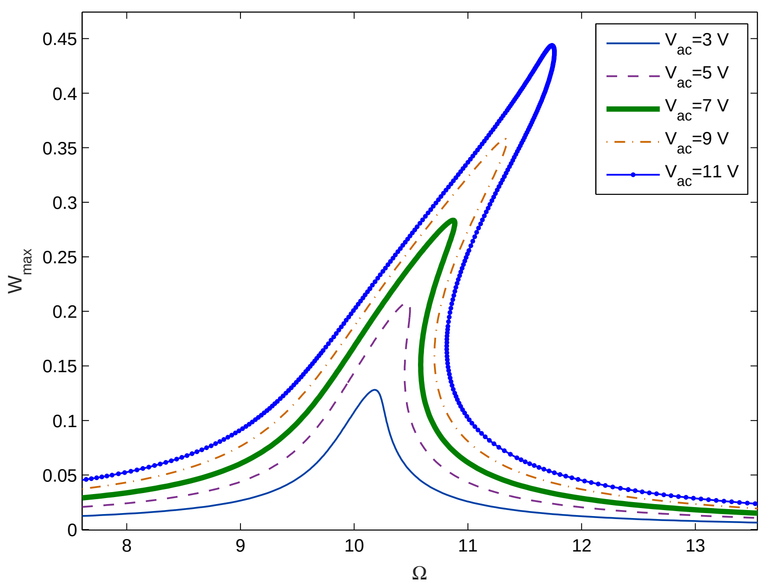

Figure 5: Forced frequency responses of the second CMUT design for $V_{dc} = 100V$ and several AC voltages.

REFERENCES

[1] T.G. Fisher, T.J. Hall, S. Panda, M.S. Richards, P.E. Barbone, J. Jiang, J. Resnick, S. Barnes, Volumetric elasticity imaging with a 2-d cmut array. *Ultrasound in medicine & biology*, **36**(6), 978–990, 2010.

[2] J. Song, S. Jung, Y. Kim, K. Cho, B. Kim, S. Lee, J. Na, I. Yang, O.-k. Kwon, D. Kim, Reconfigurable 2d cmut-asic arrays for 3d ultrasound image. In *SPIE Medical Imaging*, pages 83201A–83201A, International Society for Optics and Photonics, 2012.

[3] X. Wang, Y. Fan, W.-C. Tian, H.-J. Kwon, S. Kennerly, G. Claydon, A. May, An air-coupled capacitive micromachined ultrasound transducer for noncontact nondestructive evaluation. In *Sensors, 2007 IEEE*, pages 1464–1467, IEEE, 2007.

[4] H. Dudaicevs, M. Kandler, Y. Manoli, W. Mokwa, E. Spiegel, Surface micromachined pressure sensors with integrated cmos read-out electronics. *Sensors and Actuators A: Physical*, **43**(1), 157–163, 1994.

[5] J. Mendoza-López, C. Sánchez-López, Electromechanical performance comparison for different cmut element geometries. In *Synthesis, Modeling, Analysis and Simulation Methods and Applications to Circuit Design (SMACD), 2012 International Conference on*, pages 109–112, IEEE, 2012.

[6] B. Bayram, G.G. Yaralioglu, A.S. Ergun, B. Khuri-Yakub, Influence of the electrode size and location on the performance of a cmut [us transducer]. In *Ultrasonics Symposium, 2001 IEEE*, volume **2**, 949–952. IEEE, 2001.

[7] B. Bayram, E. Hæggstrom, G.G. Yaralioglu, B.T. Khuri-Yakub, A new regime for operating capacitive micromachined ultrasonic transducers. *Ultrasonics, Ferroelectrics, and Frequency Control, IEEE Transactions on*, **50**(9), 1184–1190, 2003.

[8] A. Lohfink, P.-C. Eccardt, Linear and nonlinear equivalent circuit modeling of cmuts. *Ultrasonics, Ferroelectrics, and Frequency Control, IEEE Transactions on*, **52**(12), 2163–2172, 2005.

[9] W.P. Mason, *Electromechanical transducers and wave filters*. D. Van Nostrand Co., 1948.

[10] O. Ahrens, A. Buhrdorf, D. Hohlfeld, L. Tebje, J. Binder, Fabrication of gap-optimized cmut. *Ultrasonics, Ferroelectrics, and Frequency Control, IEEE Transactions on*, **49**(9), 1321–1329, 2002.

[11] G.W. Vogl, A.H. Nayfeh, Primary resonance excitation of electrically actuated clamped circular plates. *Nonlinear Dynamics*, **47**(1-3), 181–192, 2007.

[12] A.H. Nayfeh, P.F. Pai, *Linear and nonlinear structural mechanics*. John Wiley & Sons, 2008.

[13] B. Cochelin, C. Vergez, A high order purely frequency-based harmonic balance formulation for continuation of periodic solutions. *Journal of sound and vibration*, **324**(1), 243–262, 2009.

[14] N. Kacem, S. Hentz, D. Pinto, B. Reig, V. Nguyen, Nonlinear dynamics of nanomechanical beam resonators: improving the performance of NEMS-based sensors. *Nanotechnology*, **20**(27), 275501, 2009.

[15] N. Kacem, S. Hentz, Bifurcation topology tuning of a mixed behavior in nonlinear micromechanical resonators. *Applied Physics Letters*, **95**(18), 183104, 2009.

[16] N. Kacem, J. Arcamone, F. Perez-Murano, S. Hentz, Dynamic range enhancement of nonlinear nanomechanical resonant cantilevers for high sensitive NEMS gas/mass sensors applications. *Journal of Micromechanics and Microengineering*, **20**(4), 045023, 2010.

[17] N. Kacem, S. Baguet, R. Dufour, S. Hentz, Stability control of nonlinear micromechanical resonators under simultaneous primary and superharmonic resonances. *Applied Physics Letters*, **98**(19), 193507, 2011.

APPENDIX

The reduced order model presented in this paper is defined as:

$$M(\eta)\ddot{\eta} + 2cM(\eta)\dot{\eta} + N(\eta)\eta = P(\eta) + v^2(t)L$$

$$\begin{aligned}
&M(\eta) = [M_{qs}(\eta)] = [\delta_{qs} - 2\eta_i A_{isq} + \eta_i\eta_j B_{ijsq}]\\
&N(\eta) = [N_{qs}(\eta)] = [\Omega_q^2\delta_{qs} - 2\Omega_q^2\eta_i A_{isq} + \Omega_q^2\eta_i\eta_j B_{ijsq}]\\
&P(\eta) = [P_q(\eta)] = \{\beta[\eta_m\eta_n\eta_p\left(C_{1mnpq} + \tfrac{1+\nu}{1-\nu}C_{2mnpq}\right) + 2\eta_i\eta_m\eta_n\eta_p\left(D_{1mnpq} + \tfrac{1+\nu}{1-\nu}D_{2mnpq}\right)\\
&-\eta_i\eta_j\eta_m\eta_n\eta_p\left(E_{1mnpq} + \tfrac{1+\nu}{1-\nu}E_{2mnpq}\right)] - \tau\eta_m F_{mq} + 2\tau\eta_i\eta_m G_{imq} - \tau\eta_i\eta_j\eta_m H_{ijmq}\\
&+I_q - 2\eta_i J_{iq} + \eta_i\eta_i K_{ijq}\}\\
&L = \{L_q\}
\end{aligned}$$

where

$$\begin{aligned}
A_{imq} &= \int_0^1 r\phi_i\phi_m\phi_q dr & B_{ijmq} &= \int_0^1 r\phi_i\phi_j\phi_m\phi_q dr & C_{1mnpq} &= \int_0^1 \phi_q'\phi_m'\varphi_{1np} dr\\
C_{2mnpq} &= \int_0^1 \phi_q'\phi_m'\varphi_{2np} dr & D_{1imnpq} &= \int_0^1 (\phi_i\phi_q)'\phi_m'\varphi_{1np} dr & D_{2imnpq} &= \int_0^1 (\phi_i\phi_q)'\phi_m'\varphi_{2np} dr\\
E_{1ijmnpq} &= \int_0^1 (\phi_i\phi_j\phi_q)'\phi_m'\varphi_{2np} dr & E_{2ijmnpq} &= \int_0^1 (\phi_i\phi_j\phi_q)'\phi_m'\varphi_{2np} dr & F_{mq} &= \int_0^1 r\phi_m'\phi_q' dr\\
H_{ijmq} &= \int_0^1 r\phi_m'(\phi_i\phi_j\phi_q)' dr & I_q &= \int_0^1 Fr\phi_q dr & J_{iq} &= \int_0^1 Fr\phi_i\phi_q dr\\
K_{ijq} &= \int_0^1 Fr\phi_i\phi_j\phi_q dr & L_q &= \int_0^1 r\phi_q dr
\end{aligned}$$

with

$$\varphi_{1mn}(r) = \frac{1}{4r}\int_0^r \xi\phi_m'\phi_n' d\xi + \frac{r}{4}\int_r^1 \frac{\phi_m'\phi_n'}{\xi} d\xi \qquad \varphi_{2mn}(r) = \frac{r}{4}\int_0^1 \xi\phi_m'\phi_n' d\xi$$